Population-based analysis of cell penetrating peptide uptake using a microfluidic droplet trapping array

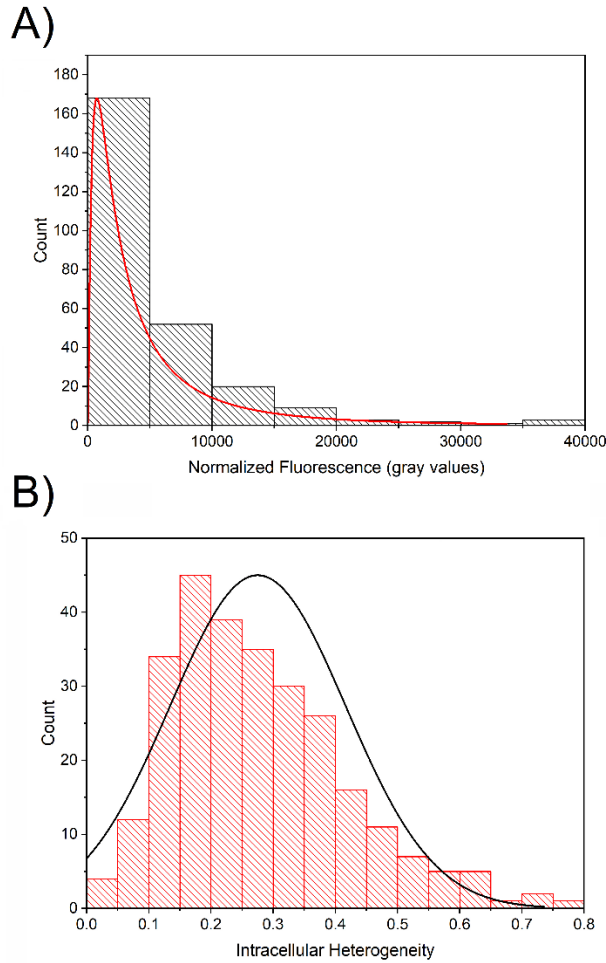Nora Safa, Manibarathi Vaithiyanathan, Shayan Sombolestani, Seleipiri Charles, Adam T. Melvin

Fig. S1 Population distribution of OWRWR peptide internalization and intracellular heterogeneity (A) Uptake of 50 µM OWRWR peptide solution in HeLa cells demonstrating logarithmic normal distribution (n=539, r^2=0.65, *p<0.05*) and (B) Observed intracellular heterogeneity (COV) of 50 µM OWRWR peptide solution in HeLa cells demonstrating normal distribution (n=274, r^2=0.92, p<0.0000001)
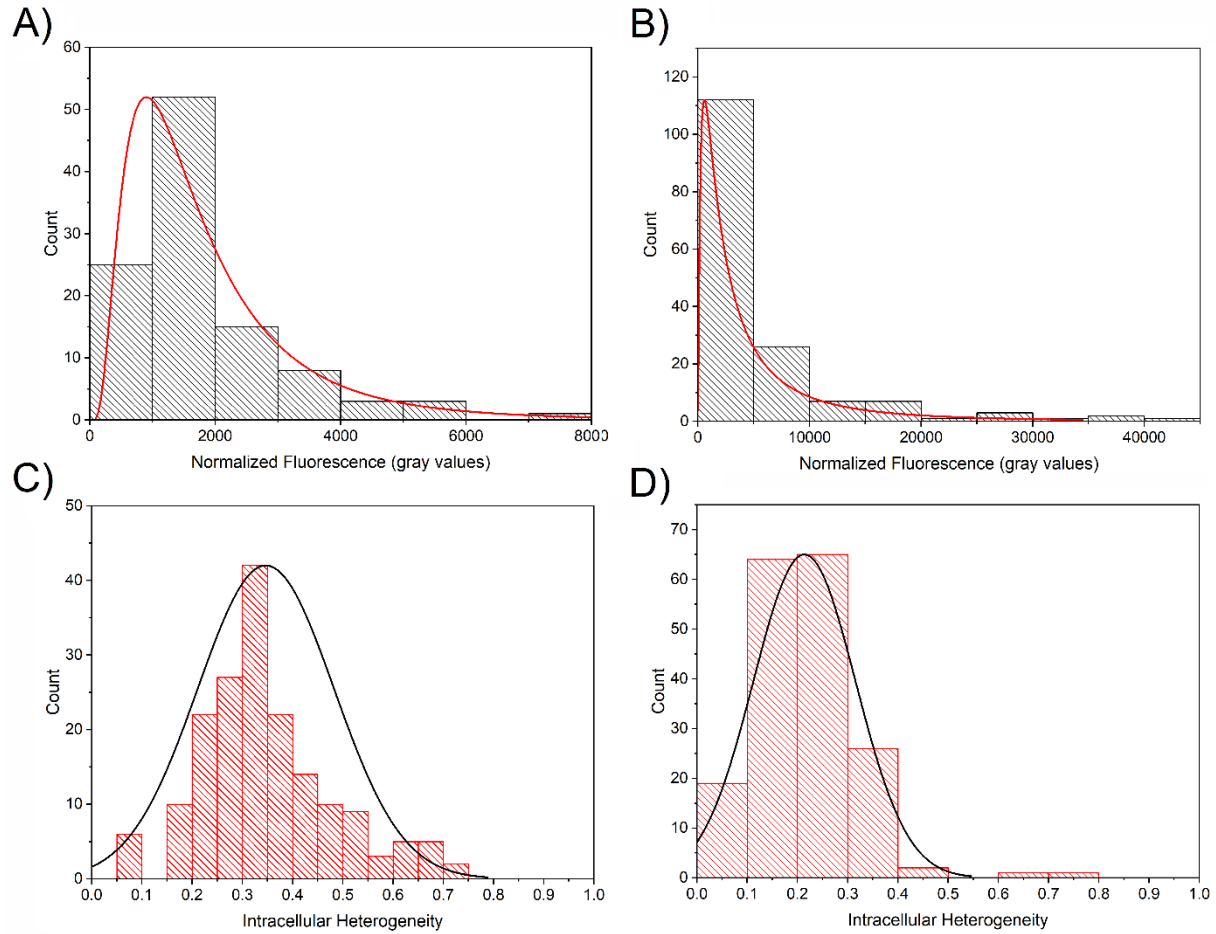
Fig. S2 Population distributions of RWRWR peptide internalization and intracellular heterogeneity. Uptake of (A) 10 µM RWRWR peptide solution in HeLa cells demonstrating logarithmic normal distribution (n=177, r^2=0.99, *p<0.00001*) and (B) 50 µM RWRWR peptide solution in HeLa cells demonstrating logarithmic normal distribution (n=178, r^2=0.91, *p<0.002*). (C) Observed intracellular heterogeneity (COV) of (C) 10 µM RWRWR peptide solution in HeLa cells demonstrating normal distribution (n=177, r^2=0.91, *p<0.000001*) and (D) 50 µM RWRWR peptide solution in HeLa cells demonstrating normal distribution (n=178, r^2=0.99, *p<00001*)
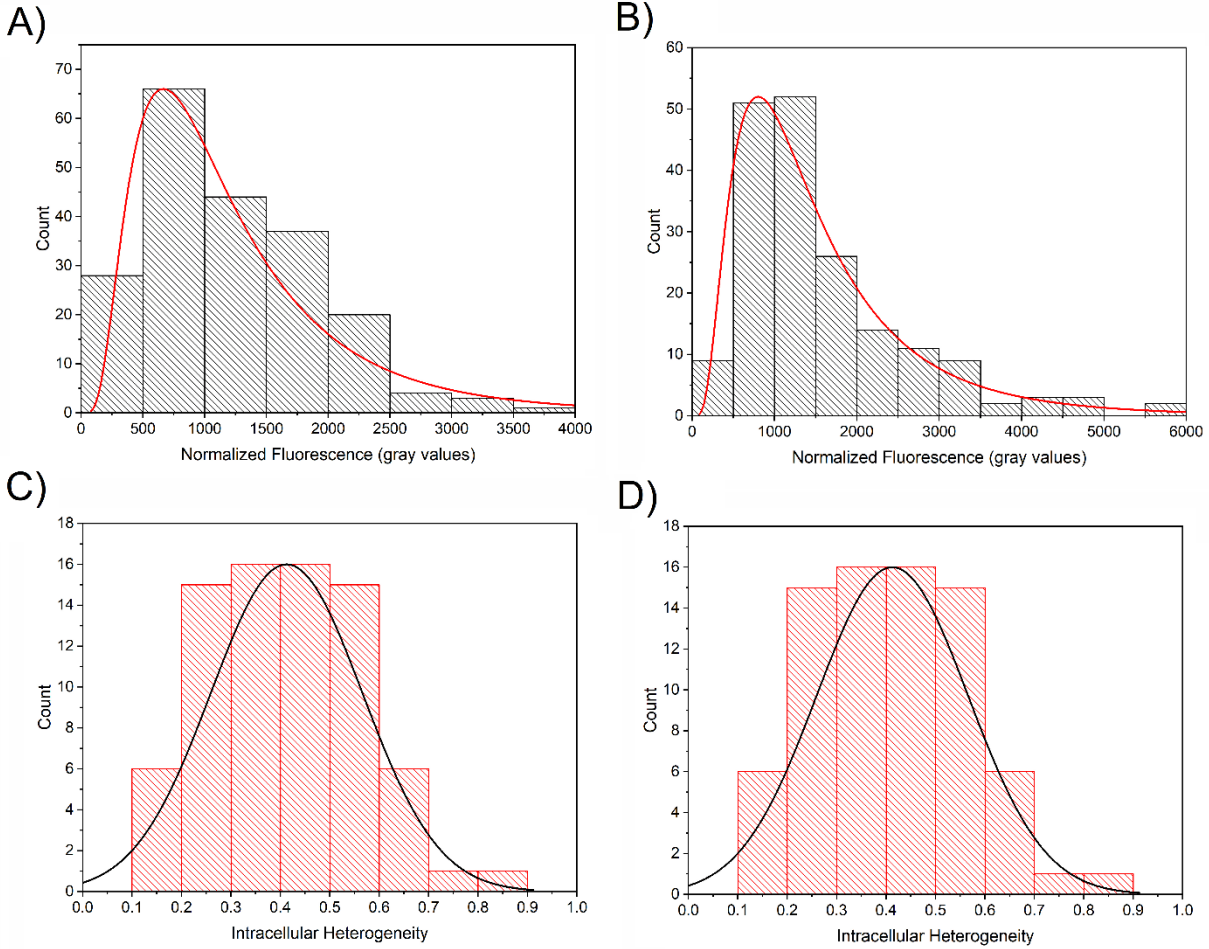
Fig. S3 Population distributions of TAT peptide internalization and intracellular heterogeneity. Uptake of (A) 10 μM TAT peptide solution in HeLa cells demonstrating logarithmic normal distribution (n=98, r^2=0.98, *p<0.0005*) and (B) 50 μM TAT peptide solution in HeLa cells demonstrating logarithmic normal distribution (n=180, r^2=0.98, *p<0.0000001*). (C) Observed intracellular heterogeneity (COV) of (C) 10 μM TAT peptide solution in HeLa cells demonstrating normal distribution (n=98, r^2=0.95, *p<0.001*) and (D) 50 μM TAT peptide solution in HeLa cells demonstrating normal distribution (n=180, r^2=0.95, *p<0.000001*)
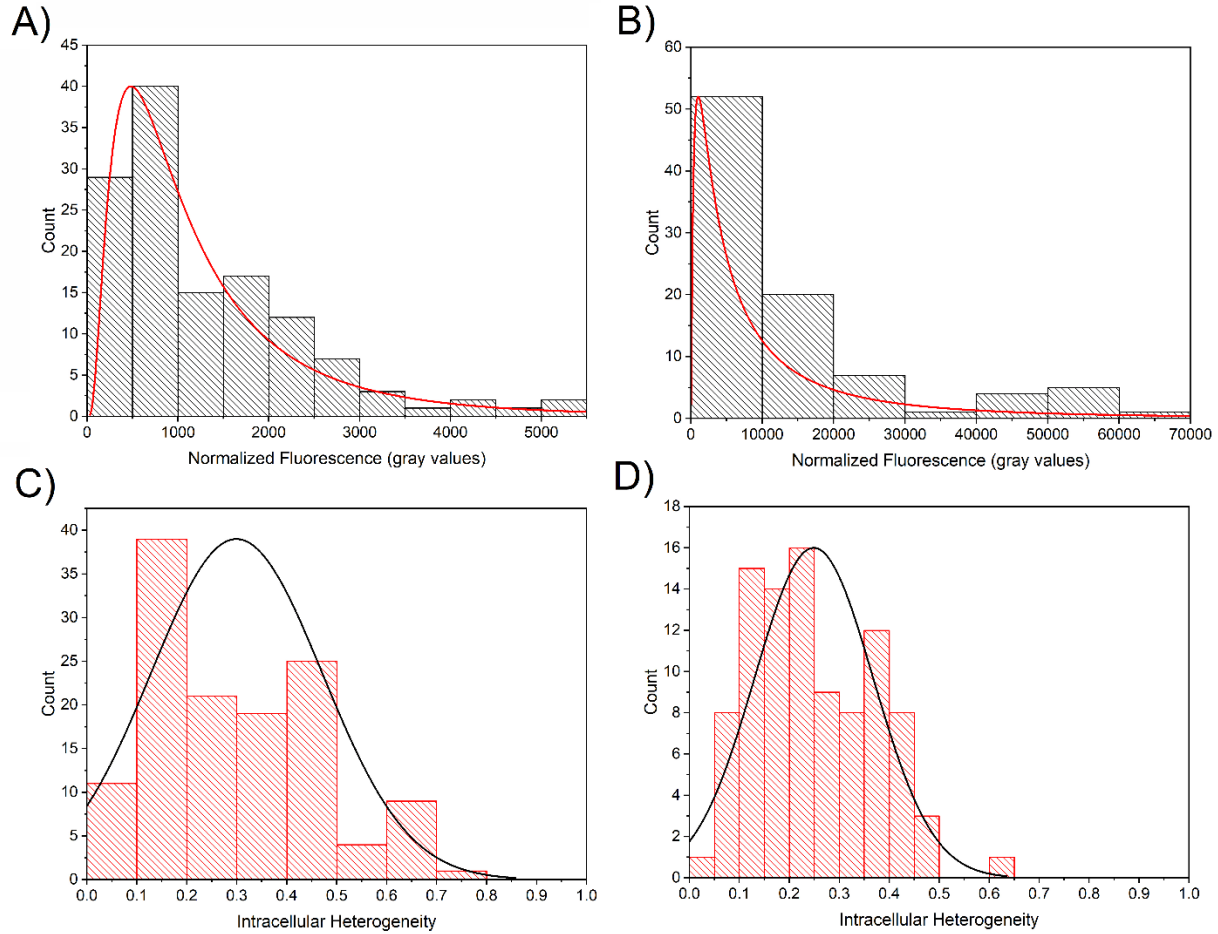
Fig. S4 Population distributions of ARG peptide internalization and intracellular heterogeneity Uptake of (A) 10 µM ARG peptide solution in HeLa cells demonstrating logarithmic normal distribution (n=129, r^2=0.94, *p<0.00001*) and (B) 50 µM ARG peptide solution in HeLa cells demonstrating logarithmic normal distribution (n=95, r^2=0.99, *p<0.0005*). (C) Observed intracellular heterogeneity (COV) of (C) 10 µM ARG peptide solution in HeLa cells demonstrating normal distribution (n=129, r^2=0.62, *p<0.05*) and (D) 50 µM ARG peptide solution in HeLa cells demonstrating normal distribution (n=95, r^2=0.80, *p<0.000005*)
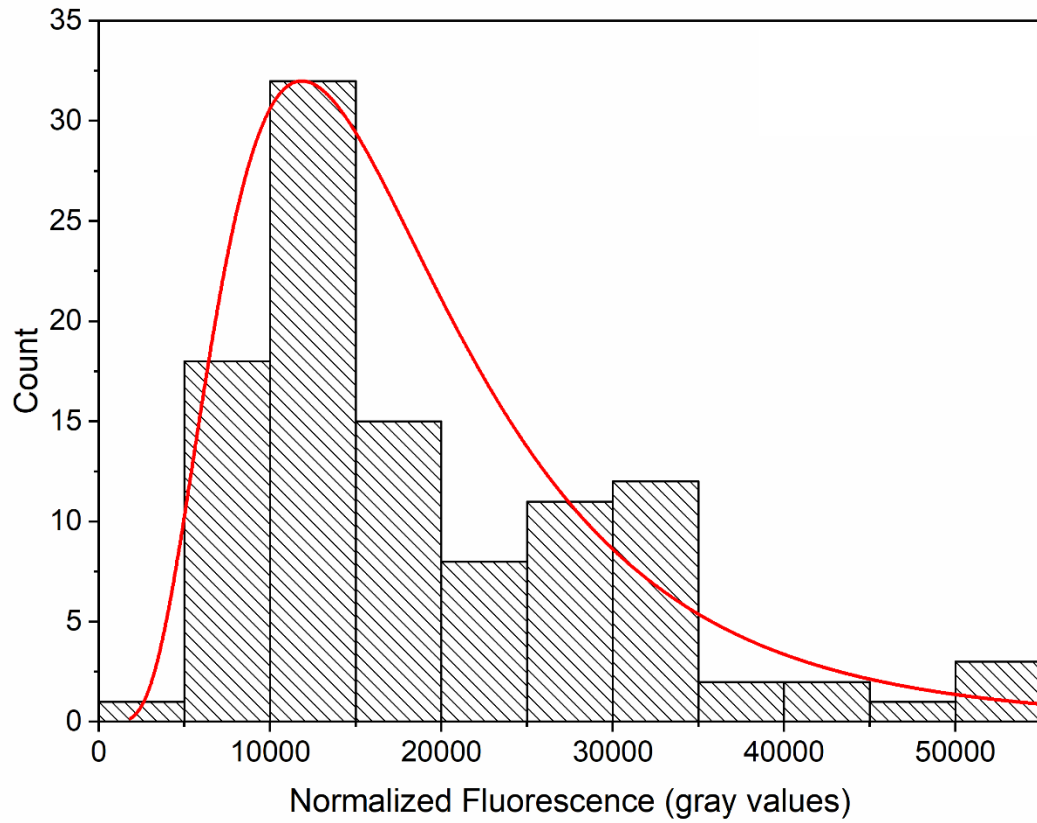
Fig. S5 Population distribution of intracellular fluorescence in GFP-expressing HeLa cells. The distribution histogram demonstrates a logarithmic normal trend as mathematically (n=105, r^2=0.86, *p<0.0005*)
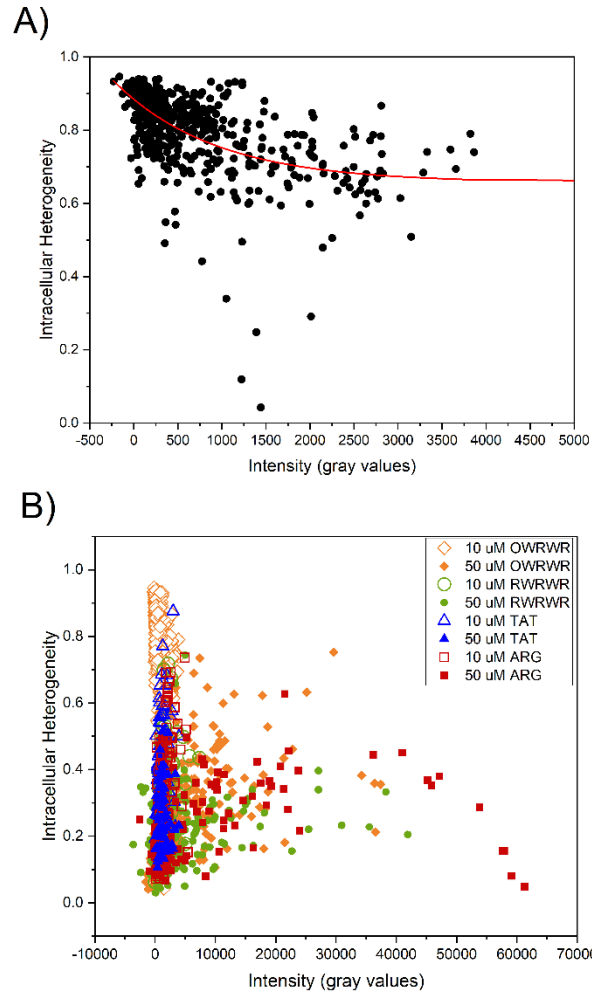
Fig. S6 Correlation between intracellular peptide distribution and CPP uptake efficiency in single-cell level (A) A correlation between intracellular heterogeneity (COV) and fluorescent intensity for cells incubated with 10 μM OWRWR simulated with an exponential function (n=537, *p<0.0001*). (B) Comparison of the single cell data of the intracellular heterogeneity and the median cellular fluorescence intensity for the entire population of HeLa cells analyzed

Table S1 Deterministic indices testing the goodness of hierarchical clustering

	Connectivity	Dunn	Silhouette
10 μM RWRWR	5.49	0.06	0.67
50 μM RWRWR	12.52	0.04	0.70
10 μM OWRWR	12.02	0.01	0.65
50 μM OWRWR	11.78	0.02	0.68
10 μM TAT	7.28	0.05	0.61
50 μM TAT	16.39	0.03	0.61
10 μM ARG	8.62	0.03	0.66
50 μM ARG	13.76	0.10	0.68

Connectivity index, Dunn index, and Silhouette width values for assessing the goodness of the clustering in terms of compactness, connectedness, and separation of the cluster partitions.